RESEARCH ARTICLE

Physical Layer Security Enhancement via IRS Based on PD-NOMA and Cooperative Jamming

AFSHIN SOUZANI[1], MOHAMMAD ALI POURMINA[1], PAEIZ AZMI[2], (Senior Member, IEEE), AND MOHAMMAD NASER-MOGHADASI[1]

[1]Department of Electrical and Computer Engineering, Science and Research Branch, Islamic Azad University, Tehran 1477893855, Iran
[2]Department of Electrical and Computer Engineering, Tarbiat Modares University, Tehran 14115, Iran

Corresponding author: Mohammad Ali Pourmina (pourmina@srbiau.ac.ir)

ABSTRACT Intelligence reconfigurable surfaces (IRS) have attracted attention due to their ability to create an intelligent and controllable wireless propagation environment for supporting an efficient, and secure design. Security and privacy protection are fundamental requirements based on the eavesdropping attacks in wireless networks. Physical layer security (PLS) is an important technique that guarantees information-theoretic security regardless of the computational capability of eavesdropping. In addition, the non-orthogonal multiple access (NOMA) as a transmission technique supports higher spectral efficiency. With the aim of increasing the secrecy rate (SR) and providing a performance analysis of IRS-based NOMA physical layer security, we propose a practical scenario equipped with IRS-assisted NOMA, containing obstacles that cause no existing direct link between the base station (BS), users, and an eavesdropper. Despite the presence of obstacles between the IRS to the second user, the first user acts as an amplifier and forwarder (AF) relay for device-to-device (D2D) communication. An eavesdropper tracks the transmitting signals in two phases: IRS to the first user, and the first user to the second user. Therefore, the second user broadcast a cooperative jamming signal which is known for the first user. To analyze the proposed system model, we obtain a closed form for the ergodic secrecy rate that numerical results reveal that increasing the elements of the IRS can enhance it. Finally, we compare the performance of the orthogonal multiple access (OMA) and NOMA in the proposed system model, which that shows the NOMA can provide a 50% more ergodic secrecy rate compared to the OMA.

INDEX TERMS Intelligent reflecting surface (IRS), non-orthogonal multiple access (NOMA), physical layer security (PLS), cooperative jammer.

I. INTRODUCTION

Due to the broadcast nature of wireless communications, the signal sent by the transmitter to the main receiver will also be received by surrounding users, including unauthorized ones, which means that this signal can be eavesdropped on by other users. Therefore, this communication is vulnerable. It is especially challenging in the fifth-generation wireless network (5G) with many connected devices, so establishing security in such systems is of particular importance. To tackle

these problems, physical layer security (PLS) techniques have emerged as a promising solution for complementing or even replacing cryptographic approaches [1].

In recent years, NOMA schemes have received significant attention to meet the challenging requirements for 5G wireless communications, such as high spectral efficiency and massive connectivity. Moreover, by using NOMA technology, the source will transmit signals to different users with different transmission power. That would lead to increasing the system's capacity. Since the non-orthogonal power range is selected in this work, there is an interference between users, causing multiple access interference problems.

Therefore, NOMA employs successive interference cancellation (SIC) technology to solve multiple access interference on the receiver. When a receiver uses the SIC method, it can obtain its signal by removing the others signals from the received signal, which is based on the difference between the power level of the different users' signals [3], [4].

Another important technology that is proposed for the next generation of cellular telecommunications is the intelligent reflecting surfaces (IRS). IRS provides various features and benefits have has received much attention for the fifth and sixth-generation mobile networks such as controlling, transmitting, and directing the signal to the desired directions, cost-effectiveness, increasing the acceptable connection, and increasing the security of the transmitted data, [5], [6], [7]. The design, construction, and physical implementation of IRS can be in the form of a fuzzy array or an antenna array that works as passive elements and can change the phase of the received signal. Employing these elements can improve the quality of the user's signal and at the same time weaken the quality of the signal that the eavesdropper receives. IRSs can reflect or detect the signals that an adjustable phase change has distorted. Signals reflected by the IRS to the receiver increase the strength of the received signal and can also cause the signal to propagate only in the direction of the main receiver. Therefore, they significantly increase the wireless network's performance without deploying additional active transmitters/relays.

In [8], the authors propose an IRS-aided NOMA network, where a BS supports a cell-center user as well as a cell-edge user with an eavesdropper which is close to the cell-edge users. It is assumed there isn't a direct link between BS and cell-edge user. Hence, the IRS establishes the communication link between BS and cell-edge user, for evaluating both the secrecy outage probability (SOP) and the average secrecy capacity (ASC). The authors in [9], propose an overview of NOMA, the advantages of IRS, and promising realizations of PLS in IRS-NOMA networks. Additionally, they illustrate two security scenarios in IRS-NOMA networks: 1) the artificial jamming-aided joint beamforming scheme for the external eavesdropping, and 2) the joint precoding and reflecting beamforming scheme for the internal untrusted user. Deploying the IRS to enhance the physical layer security in NOMA is proposed in [10]. In addition, the maximization of the secrecy sum rate of IRS-assisted multiple-input multiple-output (MIMO) NOMA has been covered in the presence of an eavesdropper. The problem formulation has a non-convex constraint, which is solved by rotating matrices and applying the particle swarm algorithm for global optimization.

One of the important notes about IRSs is that they allow the signal to be fully formed and controlled, hence, this technique can prevent the signal from being distorted by environmental objects that are distributed throughout the network. Another advantage of using an IRS is to prevent eavesdroppers from accessing the transmitted signal.

However, even with IRS, due to the high mobility of users in the network and the presence of obstacles such as buildings, trees, and machines, it is possible that the received signal is not recognizable for some users. To tackle this problem, a common solution is adding new paths to protect the communication channel. For example, in areas with very many obstacles, the amplify and forward relay (AF) or legitimate network users can be utilized to send weak signals to the destination after amplification [11], [12]. The authors in [13], propose the two-hop relaying PLS system combined with an untrusted full-duplex relay. With the aim of preventing the untrusted relay from decoding the source information, it's assumed the receiver generates artificial noise. Also, the lower bound of the ergodic secrecy rate (ESR) is expressed.

In [14], the authors have evaluated the secrecy capacity when the source is equipped with multiple antennas and it the channel state information (CSI) of the user channel is known at the jammer. In [15], the authors studied optimal power allocation between data signals and artificial noise. They obtained a relationship for confidential capacity in environments with fast fading. The authors in [16] showed that when the eavesdroppers are not collaborating to extract messages, the uniform distribution of power between the information signal and artificial noise will have a near-optimal solution. They also showed that when the number of eavesdroppers increases, the jammer should injects artificial noise with high power. The security of users' data are important issues in the next generation of mobile telecommunication, hence, the utilization of IRS to create physical layer security has been highly considered by researchers and has been studied and evaluated in various fields. In [17], the authors study the security performance of a SISO network that uses an IRS-assisted UAV scheme derived where the outage probability, average bit error rate (BER), and average capacity. To solve the problem of optimization and convexity in [18], the authors divided the problem into two sub-problems and proposed an iterative algorithm.

The study of maximizing secrecy rates in IRS-based MIMO and multiple-input single-output (MISO) networks has been studied in [19], [20], and [21], respectively. For example, in [21] maximizing secrecy rates are performed for both the known and unknown CSI. In [22], the authors examined the security of the physical layer of massive MIMO systems in the presence of eavesdroppers. In [23], the authors have compared the network efficiency in the case of using IRS with the mode of using DF relay mode and checked the number of IRS reflective elements in a single-input single-output (SISO) network. The authors' goal in [24] is to increase the total ESR in large-scale MIMO systems, and it is assumed that the eavesdroppers are equipped with multiple antennas and are randomly distributed around the transmitter. It is also assumed that all channels have Rician distribution. In this paper [24], the authors designed the jamming signal in a network that is equipped with a large number of antennas. As well as, they studied two directional and uniform jammers

and the secure message is transmitted to a legitimate destination by employing the beamforming technique. At the same time, by using artificial noise in other directions, the secrecy rate (SR) increase. The authors also evaluated the SOP by defining the suspicious area (where eavesdroppers are likely to be present). They also introduced the concept of Secrecy Outage Region (SOR). The SOR area is the area where the outage of confidentiality of information transmission occurs.

As mentioned above the advantages of using IRS-assisted NOMA to improve the secrecy rate, our main contributions to this paper are summarized as follows:

- We propose a system consisting of a multiple-antenna BS and two single-antenna users with no direct link between them due to existing obstacles. IRS-assisted NOMA which is composed of N reflecting elements is utilized to establish communication links between BS and the first user. Since the second user hasn't direct links due to an obstacle with BS and IRS, the first user plays the role of AF relay to transmit the second user's data, while ensuring the security of the second user's information, too.
- In addition, to improve the significant secrecy rate, the second user broadcasts the jamming signal which is known for the first user [12] and causes degrading the eavesdropping rate.
- We obtain a closed-form for ergodic secrecy rate, to analyze the proposed system model. Also, we investigate the performance of our proposed system model on some different scenarios jointly: variation of the level of transmitter SNR and the number of IRS elements, variation of the level of transmitter SNR, and the eavesdropper's movement.
- We evaluate the performance of OMA compared to NOMA in the proposed system model. We show that the NOMA can provide a 50% more ergodic secrecy rate compared to the OMA technique.
- Finally, in the numerical results, we demonstrate that increasing the number of reflective elements of the IRS can increase the ergodic secrecy rate, due to the properties of adjusting the beam elements.

The remainder of the paper is organized as follows. In Section II, the system and signal models are presented. In Section III, solutions of problems are investigated used to improve the ESR presents the simulation results in Section IV. Finally, the concluding remarks are expressed in Section V.

Notation: scalars, vectors, and matrices are denoted by lower case letters, bold face lower case letter, and bold face upper case letters, respectively.

II. SYSTEM MODEL

We consider a system consisting of a base station (BS or gNB) with M antennas, an IRS with N reflective elements, two users namely U_1 and U_2, and an eavesdropper namely U_{Eve}, all users and eavesdropper are equipped with one antenna and act as half-duplex, as shown in Fig. 1.
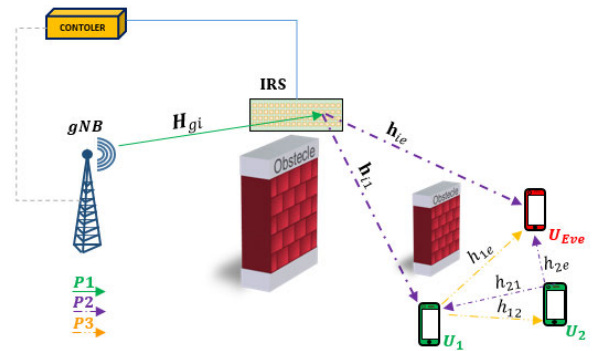

FIGURE 1. Illustration of the IRS-assisted NOMA communication system without a line of sight (LoS) links between users and multiple antenna BS, in the presence of an Eavesdropper.

In this scheme, U_1 and U_2 are near and far users, respectively. Due to the obstacles between users and the BS, there is no direct link between them. Hence, communication is possible by employing the IRS-assisted NOMA.

In addition, as shown in Fig. 1, U_2 cannot communicate with an IRS due to an obstacle. To tackle this issue, we employ a new auxiliary path to keep communication. In other words, U_1 is used as an AF relay to transmit U_2's signals. In the following, we analyze the proposed system model and calculate a closed form for ESR.

III. CLOSED-FORM SOLUTIONS
A. SIGNAL REPRESENTATION

According to the proposed system model, the transmission is done in three phases. In phase 1, BS transmits the data signal x with p_s power transmission. Note x is combined x_1 and x_2, where x_1 and x_2 are data signals for U_1 and U_2, respectively, and $E\left\{|x_1|^2\right\} = E\left\{|x_2|^2\right\} = 1$. $E\left\{.\right\}$ denotes the expectation operator. Introducing power splitting factor $\alpha \in [0, 1]$, since U_2 is further away from BS than U_1 and has worse channel conditions than U_1. As a result, the transmit signal in BS is:

$$x = f\left(\sqrt{\alpha p_s}x_1 + \sqrt{(1-\alpha)p_s}x_2\right), \qquad (1)$$

where $f \in \mathbb{C}^{M \times 1}$ is the beamforming vector which satisfies $\|f\|^2 = 1$. The received signal in the IRS in the first phase is expressed as follows:

$$y_{IRS}^{(1)} = H_{gi}x, \qquad (2)$$

where $H_{gi} \in \mathbb{C}^{N \times M}$ is the channel between BS and the IRS, and $\mathbb{C}^{N \times M}$ denotes the $N \times M$ complex-valued matrices space. In the second phase, the IRS sends the received signal to U_1. To prevent eavesdropping, U_2 simultaneously injects a jamming signal x_j with power P_j. It is assumed that the jamming signal is known at U_1 and can remove it [12]. In this phase, U_1 detects its signal after performing SIC. Accordingly, the received signal in U_1 in the second phase is expressed as follows:

$$y_{U_1}^{(2)} = \left(h_{i1}^H \Phi H_{gi}\right)x + \sqrt{P_j}x_j h_{21} + n_1^{(2)}, \qquad (3)$$

where $\boldsymbol{h}_{i1} \in \mathbb{C}^{N \times 1}$, $h_{21} \in \mathbb{C}^{1 \times 1}$ are the channel between the IRS to U_1, and U_2 to U_1, respectively. Also, $\boldsymbol{\Phi} = diag\left\{\beta_1 e^{j\varphi_1}, \dots, \beta_n e^{j\varphi_n}\right\}$ is the diagonal matrix, where $\beta_n \in [0, 1]$ and $\varphi_n \in [0, 2\pi)$ are the amplitude reflection coefficient and the phase shift of the n-th element of the IRS. $n_1^{(2)}$ is complex Gaussian noise with zero mean and variance $\sigma_{U_1}^2$. The received signal at the eavesdropper in the second phase is expressed as follows:

$$y_{\mathrm{E}}^{(2)} = \left(\boldsymbol{h}_{ie}^{H} \boldsymbol{\Phi} \boldsymbol{H}_{gi}\right) \boldsymbol{x} + \sqrt{P_j} x_j h_{2e} + n_E^{(2)}, \quad (4)$$

where $\boldsymbol{h}_{ie} \in \mathbb{C}^{N \times 1}$, $h_{2e} \in \mathbb{C}^{1 \times 1}$ are the channel between the IRS to U_{Eve}, and U_2 to the U_{Eve}. $n_E^{(2)}$ is the complex Gaussian noise with zero mean and variance σ_E^2 at the U_{Eve} in phase 2.

In the third phase, U_1 appears as AF relay with gain G. It amplifies and transmits the received signal in the previous phase to U_2. Therefore, the received signal at U_2 in the third phase is equal to:

$$y_{U_2}^{(3)} = G h_{12} y_{U_1}^{(2)} + n_2^{(3)}, \quad (5)$$

where $h_{12} \in \mathbb{C}^{1 \times 1}$ is the channel between U_1 and U_2 and $G = \sqrt{\dfrac{P_r}{p_s \left|\left(\boldsymbol{h}_{i1}^{H} \boldsymbol{\Phi} \boldsymbol{H}_{gi}\right) \boldsymbol{f}\right|^2 + P_j |h_{21}|^2 + \sigma_{U_1}^2}}$ is gain of the relay, with relay power P_r. $n_2^{(3)}$ is the complex Gaussian noise with zero mean and variance $\sigma_{U_2}^2$ at the U_2 in the third phase of communication. Also, the received signal at the U_{Eve} in the third phase is:

$$y_{\mathrm{E}}^{(3)} = G h_{1e} y_{U_1}^{(2)} + n_E^{(3)}, \quad (6)$$

where $h_{1e} \in \mathbb{C}^{1 \times 1}$ is the channel between U_1 and the U_{Eve}, and $n_E^{(3)}$ is the complex Gaussian noise with zero mean and variance σ_E^2 at the U_{Eve} in the third phase.

Considering (3), (4) the signal to noise ratio (SNR) at U_1 and the signal to interference plus noise ratio (SINR) at U_{Eve} in the second phase are calculated, respectively, as:

$$\gamma_{U_1}^{(2)} = \frac{\alpha p_s \left|\left(\boldsymbol{h}_{i1}^{H} \boldsymbol{\Phi} \boldsymbol{H}_{gi}\right) \boldsymbol{f}\right|^2}{\sigma_{U_1}^2}, \quad (7)$$

$$\gamma_{E}^{(2)} = \frac{p_s \left|\left(\boldsymbol{h}_{ie}^{H} \boldsymbol{\Phi} \boldsymbol{H}_{gi}\right) \boldsymbol{f}\right|^2}{P_j |h_{2e}|^2 + \sigma_E^2}. \quad (8)$$

Also, based on (5) and (6) SINR at U_2 and the U_{Eve} in the third phase is given by, respectively, as:

$$\gamma_{U_2}^{(3)} = \frac{G^2 (1-\alpha) p_s \left|\left(\boldsymbol{h}_{i1}^{H} \boldsymbol{\Phi} \boldsymbol{H}_{gi}\right) \boldsymbol{f}\right|^2 |h_{12}|^2}{G^2 \left(\alpha p_s \left|\left(\boldsymbol{h}_{i1}^{H} \boldsymbol{\Phi} \boldsymbol{H}_{gi}\right) \boldsymbol{f}\right|^2 + \sigma_{U_1}^2\right) |h_{12}|^2 + \sigma_{U_2}^2}, \quad (9)$$

$$\gamma_{E}^{(3)} = \frac{G^2 p_s \left|\left(\boldsymbol{h}_{i1}^{H} \boldsymbol{\Phi} \boldsymbol{H}_{gi}\right) \boldsymbol{f}\right|^2 |h_{1e}|^2}{G^2 \left(P_j |h_{21}|^2 + \sigma_{U_1}^2\right) |h_{1e}|^2 + \sigma_E^2}. \quad (10)$$

B. ERGODIC SECRECY RATE ANALYSIS

In this section, we obtain new closed-form expression for the lower bound of ESR. Accordingly, the instantaneous sum secrecy rate (SSR) is obtained as follows [12]:

$$R_s = \frac{2}{3} [R_L - R_E]^+, \quad (11)$$

which R_L is the total legitimate rate and the R_E is the total eavesdropping rate. Also, $[x]^+ = max\{0, x\}$. The total legitimate rate is the SSR in U_1 and U_2, which is expressed as follows:

$$R_L = \log_2\left(1 + \gamma_{U_1}^{(2)}\right) + \log_2\left(1 + \gamma_{U_2}^{(3)}\right). \quad (12)$$

The total eavesdropping rate at U_{Eve} is obtained as follows:

$$R_E = \log_2\left(1 + \gamma_E^{(2)}\right) + \log_2\left(1 + \gamma_E^{(3)}\right). \quad (13)$$

According to (11)-(13), the SSR is rewrite as follows:

$$R_s = \frac{2}{3} \left[\log_2\left(1 + \gamma_{U_1}^{(2)}\right) + \log_2\left(1 + \gamma_{U_2}^{(3)}\right) \right.$$
$$\left. - \left(\log_2\left(1 + \gamma_E^{(2)}\right) + \log_2\left(1 + \gamma_E^{(3)}\right)\right)\right]^+. \quad (14)$$

The lower bound of R_S is calculated as follows

$$\bar{R}_s = E\{R_s\}, \quad (15a)$$

$$\bar{R}_s = \frac{2}{3 \ln 2} \left[\left(E\left\{\ln\left(1 + \gamma_{U_1}^{(2)}\right)\right\} + E\left\{\ln\left(1 + \gamma_{U_2}^{(3)}\right)\right\}\right)\right.$$
$$\left. - \left(E\left\{\ln\left(1 + \gamma_E^{(2)}\right)\right\} + E\left\{\ln\left(1 + \gamma_E^{(3)}\right)\right\}\right)\right]^+ \quad (15b)$$

We define some notations such as $p_s = \lambda P$, $P_r = P_j = P$, $\sigma_{U_1}^2 = \sigma_{U_2}^2 = \sigma_E^2 = \sigma^2$, $\rho = \frac{P}{\sigma^2}$, $\gamma_{ij} = \rho \|\boldsymbol{h}_{ij}\|^2$, $\gamma_{gi} = \rho \|\boldsymbol{H}_{gi}\boldsymbol{f}\|^2$, and according to the law of large numbers (LLN) $\bar{\gamma}_{ij} = \rho N \mu_{ij}$; $\gamma_{ij} \gg 1$; $\forall i, j$, where μ_{ij} is variance of $\boldsymbol{h}_{ij}$. Also, motivated by maximum ratio transmitter (MRT), we assume $\boldsymbol{\Phi} = \frac{\boldsymbol{h}_{i1}}{\|\boldsymbol{h}_{i1}\|} \boldsymbol{I}_N$, where $\boldsymbol{I}_N$ denote the Identity matrix. Hence, the SNR at U_1 in the second phase (IRS reflected signals to U_1) is simplified as:

$$\gamma_{U_1}^{(2)} = \frac{\alpha \lambda P \left|\left(\boldsymbol{h}_{i1}^{H} \boldsymbol{\Phi} \boldsymbol{H}_{gi}\right) \boldsymbol{f}\right|^2}{\sigma^2}$$
$$= \alpha \lambda \rho \left|\left(\boldsymbol{h}_{i1}^{H} \frac{\boldsymbol{h}_{i1}}{\|\boldsymbol{h}_{i1}\|} \boldsymbol{I}_N \boldsymbol{H}_{gi}\right) \boldsymbol{f}\right|^2$$
$$= \alpha \lambda \rho \left|\left(\frac{\|\boldsymbol{h}_{i1}\|^2}{\|\boldsymbol{h}_{i1}\|} \boldsymbol{H}_{gi}\right) \boldsymbol{f}\right|^2 = \alpha \lambda \rho \|\boldsymbol{h}_{i1}\|^2 \|\boldsymbol{H}_{gi}\boldsymbol{f}\|^2$$
$$= \alpha \lambda N \mu_{i1} \gamma_{gi}. \quad (16)$$

In addition, the SINR in the third phase with the assumption of $p_s = \lambda P$, $P_r = P_j = P$ is given by:

$$\gamma_{U_2}^{(3)} = \frac{G^2 (1-\alpha) \lambda P \left|\left(\boldsymbol{h}_{i1}^{H} \boldsymbol{\Phi} \boldsymbol{H}_{gi}\right) \boldsymbol{f}\right|^2 |h_{12}|^2}{G^2 \left(\alpha \lambda P \left|\left(\boldsymbol{h}_{i1}^{H} \boldsymbol{\Phi} \boldsymbol{H}_{gi}\right) \boldsymbol{f}\right|^2 + \sigma^2\right) |h_{12}|^2 + \sigma^2}$$
$$= \frac{(1-\alpha) \lambda N \mu_{i1} \gamma_{gi} \gamma_{12}}{\alpha \lambda N \mu_{i1} \gamma_{gi} \gamma_{12} + \gamma_{12} + \lambda N \mu_{i1} \gamma_{gi} + \gamma_{21} + 1}$$
$$\cong \frac{(1-\alpha) \lambda N \mu_{i1} \gamma_{gi} \gamma_{12}}{\alpha \lambda N \mu_{i1} \gamma_{gi} \gamma_{12} + \gamma_{12} + \lambda N \mu_{i1} \gamma_{gi} + \gamma_{21}}. \quad (17)$$

Moreover, SINR at the U_{Eve} in the second phase is as follows:

$$\gamma_E^{(2)} = \frac{\lambda P \left|\left(\boldsymbol{h}_{ie}^{H} \boldsymbol{\Phi} \boldsymbol{H}_{gi}\right) \boldsymbol{f}\right|^2}{P |h_{2e}|^2 + \sigma^2}$$

$$
= \frac{\frac{\lambda P}{\|\boldsymbol{h}_{i1}\|^2} \left\| \left(\boldsymbol{h}_{ie}^H \boldsymbol{h}_{i1} \boldsymbol{I}_N \boldsymbol{H}_{gi}\right) \boldsymbol{f} \right\|^2}{\sigma^2 \left(\frac{P|h_{2e}|^2}{\sigma^2} + 1 \right)}
$$

$$
= \frac{\lambda \rho \hat{h}_{e1g}}{N \mu_{i1} (\gamma_{2e} + 1)} \cong \frac{\lambda \gamma_{e1g}}{N \mu_{i1} \gamma_{2e}}, \qquad (18)
$$

where $\hat{h}_{e1g} = \left\| \left(\boldsymbol{h}_{ie}^H \boldsymbol{h}_{i1} \boldsymbol{H}_{gi}\right) \boldsymbol{f} \right\|^2$.

Furthermore, SINR at the U_{Eve} in the third phase is given by:

$$
\gamma_E^{(3)} = \frac{G^2 \lambda P \left|\left(\boldsymbol{h}_{i1}^H \boldsymbol{\Phi} \boldsymbol{H}_{gi}\right)\boldsymbol{f}\right|^2 |h_{1e}|^2}{G^2 (P|h_{21}|^2 + \sigma^2)|h_{1e}|^2 + \sigma^2}
$$

$$
= \frac{\lambda N \mu_{i1} \gamma_{gi} \gamma_{1e}}{\gamma_{21} \gamma_{1e} + \gamma_{1e} + \lambda N \mu_{i1} \gamma_{gi} + \gamma_{21} + 1}
$$

$$
\cong \frac{\lambda N \mu_{i1} \gamma_{gi} \gamma_{1e}}{\gamma_{21} \gamma_{1e} + \gamma_{1e} + \lambda N \mu_{i1} \gamma_{gi} + \gamma_{21}} \qquad (19)
$$

In the following, we obtain a lower bound for $\bar{R}_s$. By employing (15), we have:

$$
\bar{R}_s = \frac{2}{3\ln 2} E \left\{ \ln \left[\frac{\left(1 + \gamma_{U_1}^{(2)}\right)\left(1 + \gamma_{U_2}^{(3)}\right)}{\left(1 + \gamma_E^{(2)}\right)\left(1 + \gamma_E^{(3)}\right)} \right]^+ \right\}
$$

$$
= \frac{2}{3\ln 2} E \left\{ \left[\left(\ln\left(1 + \gamma_{U_1}^{(2)}\right) + \ln\left(1 + \gamma_{U_2}^{(3)}\right)\right) \right. \right.
$$

$$
\left. \left. - \left(\ln\left(1 + \gamma_E^{(2)}\right) + \ln\left(1 + \gamma_E^{(3)}\right)\right)\right]^+ \right\}
$$

$$
\geq \frac{2}{3\ln 2} \left[\underbrace{E\left\{\ln\left(1 + \gamma_{U_1}^{(2)}\right)\right\}}_{I_1} + \underbrace{E\left\{\ln\left(1 + \gamma_{U_2}^{(3)}\right)\right\}}_{I_2} \right.
$$

$$
\left. - \left(\underbrace{E\left\{\ln\left(1 + \gamma_E^{(2)}\right)\right\}}_{I_3} + \underbrace{E\left\{\ln\left(1 + \gamma_E^{(3)}\right)\right\}}_{I_4}\right) \right]^+
$$

$$
(20)
$$

Next, to obtain the lower bound $\bar{R}_s$, we should calculate I_1, I_2, I_3, and I_4. By defining $\hat{I}_1$ to $\hat{I}_4$ we have relations, Eq. (22) to (25).

$$
\bar{R}_{s(LB)} = \frac{2}{3\ln 2} \left[\hat{I}_1 + \hat{I}_2 - \left(\hat{I}_3 + \hat{I}_4\right) \right]^+ \qquad (21)
$$

$$
\hat{I}_1 \geq E \left\{ \ln\left(1 + \alpha \lambda N \mu_{i1} \gamma_{gi}\right) \right\} \qquad (22)
$$

$$
\hat{I}_2 \geq E \left\{ \ln \left(1 \right. \right.
$$

$$
\left. \left. + \frac{(1 - \alpha) \lambda N \mu_{i1} \gamma_{gi} \gamma_{12}}{\alpha \lambda N \mu_{i1} \gamma_{gi} \gamma_{12} + \gamma_{12} + \lambda N \mu_{i1} \gamma_{gi} + \gamma_{21}} \right) \right\} \qquad (23)
$$

$$
\hat{I}_3 \leq E \left\{ \ln\left(1 + \frac{\lambda \gamma_{e1g}}{N \mu_{i1} \gamma_{2e}}\right) \right\} \qquad (24)
$$

$$
\hat{I}_4 \leq E \left\{ \ln\left(1 + \frac{\lambda N \mu_{i1} \gamma_{gi} \gamma_{1e}}{\gamma_{21} \gamma_{1e} + \gamma_{1e} + \lambda N \mu_{i1} \gamma_{gi} + \gamma_{21}}\right) \right\} \qquad (25)
$$

In the following, we calculate I_1 to I_4:

1) CALCULATION OF I₁

$$
I_1 = E \left\{ \ln \left(1 + \underbrace{\alpha \lambda N \mu_{i1}}_{\beta} \underbrace{\gamma_{gi}}_{x} \right) \right\}
$$

$$
\underbrace{=}_{a_1} \int_0^\infty \ln\left(1 + \alpha \lambda N \mu_{i1} \gamma_{gi}\right) f_{\gamma_{gi}}(x) \, dx
$$

$$
\underbrace{=}_{a_2} -e^{\frac{1}{\alpha \lambda N \mu_{i1} \bar{\gamma}_{gi}}} Ei\left(-\frac{1}{\alpha \lambda N \mu_{i1} \bar{\gamma}_{gi}}\right);
$$

$$
\left\{ \left|arg\left(\alpha \lambda N \mu_{i1}\right)\right| < \pi, \, Re\left(\frac{1}{\bar{\gamma}_{gi}}\right) > 0 \right\}, \quad (26)
$$

$Ei(x)$ is the exponential integral function. Since γ_{gi} is a random variable in the range $(0, \infty)$ with the probability density function $f_{\gamma_{gi}}(x) = (1/\bar{\gamma}_{gi}) e^{-\frac{x}{\bar{\gamma}_{gi}}}$ and using the mathematical expectation proposition $E(X) = \int_{-\infty}^\infty x f_X(x) dx$, we can get the value of a_1. According to Eq (4.337.2) from the book of integrals [25] and using the following equation, the value of a_2 is obtained [25].

2) CALCULATION OF I₂

$$
I_2 = E \left\{ \ln \left(1 + \frac{(1 - \alpha) \lambda N \mu_{i1} \gamma_{gi} \gamma_{12}}{\alpha \lambda N \mu_{i1} \gamma_{gi} \gamma_{12} + \gamma_{12} + \lambda N \mu_{i1} \gamma_{gi} + \gamma_{21}} \right) \right\}
$$

$$
= E \left\{ \ln \left(\frac{\lambda N \mu_{i1} \gamma_{gi} \gamma_{12} + \gamma_{12} + \lambda N \mu_{i1} \gamma_{gi} + \gamma_{21}}{\alpha \lambda N \mu_{i1} \gamma_{gi} \gamma_{12} + \gamma_{12} + \lambda N \mu_{i1} \gamma_{gi} + \gamma_{21}} \right) \right\}
$$

$$
\cong E \left\{ \ln \left(\frac{\lambda N \mu_{i1} \gamma_{gi} \gamma_{12} + \gamma_{21}}{\alpha \lambda N \mu_{i1} \gamma_{gi} \gamma_{12} + \gamma_{21}} \right) \right\}
$$

$$
= E \left\{ \ln \left(\gamma_{21} + \lambda N \mu_{i1} \gamma_{gi} \gamma_{12} \right) \right\}
$$

$$
- E \left\{ \ln \left(\gamma_{21} + \alpha \lambda N \mu_{i1} \gamma_{gi} \gamma_{12} \right) \right\}
$$

$$
= E \left\{ \ln \left(\gamma_{21} \left(1 + \lambda N \mu_{i1} \frac{\gamma_{gi} \gamma_{12}}{\gamma_{21}} \right) \right) \right\}
$$

$$
- E \left\{ \ln \left(\gamma_{21} \left(1 + \alpha \lambda N \mu_{i1} \frac{\gamma_{gi} \gamma_{12}}{\gamma_{21}} \right) \right) \right\} \qquad (27)
$$

Finally (27) is simplified as:

$$
I_2 = \underbrace{E \left\{ \ln \left(1 + \lambda N \mu_{i1} \frac{\gamma_{gi} \gamma_{12}}{\gamma_{21}} \right) \right\}}_{I_{2(1)}}
$$

$$
- \underbrace{E \left\{ \ln \left(1 + \alpha \lambda N \mu_{i1} \frac{\gamma_{gi} \gamma_{12}}{\gamma_{21}} \right) \right\}}_{I_{2(2)}} \qquad (28)
$$

The detail of calculation $I_{2(1)}$, and $I_{2(2)}$ are expressed in Appendix A, which are equivalent to (29), and (30) respectively, as:

$$
I_{2(1)} = \int_0^\infty \frac{\lambda N \mu_{i1} \left(\left(e^{\frac{\bar{\gamma}_{21} z}{2 \bar{\gamma}_{gi} \bar{\gamma}_{12}}} W_{-1, -\frac{1}{2}} \left(\frac{\bar{\gamma}_{21} z}{\bar{\gamma}_{gi} \bar{\gamma}_{12}} \right) \right) \right)}{1 + \lambda N \mu_{i1} z} dz;
$$

$$
\left\{ \left| arg \left(\frac{\bar{\gamma}_{gi}}{\bar{\gamma}_{21}} \right) \right| < \pi, \, Re(2) > Re(1) > 0 \right\} \qquad (29)
$$

$$I_{2(2)} = \int_0^\infty \frac{\alpha\lambda N\mu_{i1}\left(\left(e^{\frac{\bar{\gamma}_{21}z}{2\bar{\gamma}_{gi}\bar{\gamma}_{12}}} W_{-1,-\frac{1}{2}}\left(\frac{\bar{\gamma}_{21}z}{\bar{\gamma}_{gi}\bar{\gamma}_{12}}\right)\right)\right)}{1+\alpha\lambda N\mu_{i1}z}dz;$$
$$\left\{\left|arg\left(\frac{\bar{\gamma}_{gi}}{\bar{\gamma}_{21}}\right)\right| < \pi, Re(2) > Re(1) > 0\right\} \quad (30)$$

Therefore, according to (29), and (30), we rewrite (28) as:

$$I_2 = I_{2(1)} - I_{2(2)}$$
$$= \int_0^\infty \frac{\lambda N\mu_{i1}\left(\left(e^{\frac{\bar{\gamma}_{21}z}{2\bar{\gamma}_{gi}\bar{\gamma}_{12}}} W_{-1,-\frac{1}{2}}\left(\frac{\bar{\gamma}_{21}z}{\bar{\gamma}_{gi}\bar{\gamma}_{12}}\right)\right)\right)}{1+\lambda N\mu_{i1}z}dz$$
$$- \int_0^\infty \frac{\alpha\lambda N\mu_{i1}\left(\left(e^{\frac{\bar{\gamma}_{21}z}{2\bar{\gamma}_{gi}\bar{\gamma}_{12}}} W_{-1,-\frac{1}{2}}\left(\frac{\bar{\gamma}_{21}z}{\bar{\gamma}_{gi}\bar{\gamma}_{12}}\right)\right)\right)}{1+\alpha\lambda N\mu_{i1}z}dz;$$
$$\left\{\left|arg\left(\frac{\bar{\gamma}_{gi}}{\bar{\gamma}_{21}}\right)\right| < \pi, Re(2) > Re(1) > 0\right\} \quad (31)$$

3) CALCULATION OF I_3

Based on (24), and Appendix B, I_3 is calculated as follows:

$$I_3 = E\left\{\ln\left(1+\frac{\lambda\gamma_{e1g}}{N\mu_{i1}\gamma_{2e}}\right)\right\}$$
$$= -\frac{\frac{\bar{\gamma}_{e1g}}{\bar{\gamma}_{2e}}\left(\ln\left(\frac{\bar{\gamma}_{e1g}}{\bar{\gamma}_{2e}}\right)-\ln\left(\frac{N\mu_{i1}}{\lambda}\right)\right)}{-\frac{\bar{\gamma}_{e1g}}{\bar{\gamma}_{2e}}+\frac{N\mu_{i1}}{\lambda}};$$
$$\frac{\bar{\gamma}_{e1g}}{\bar{\gamma}_{2e}} > 0, \quad \frac{N\mu_{i1}}{\lambda} > 0 \quad (32)$$

4) CALCULATION OF I_4:

According to (25), and Appendix C, I_4 is calculated as:

$$I_4 = E\left\{\ln\left(1+\frac{\lambda N\mu_{i1}\gamma_{gi}\gamma_{1e}}{\gamma_{21}\gamma_{1e}+\gamma_{1e}+\lambda N\mu_{i1}\gamma_{gi}+\gamma_{21}}\right)\right\}$$
$$= \underbrace{E\left\{\ln\left(1+\lambda N\mu_{i1}\frac{\gamma_{gi}}{\gamma_{21}}\right)\right\}}_{I_{4(1)}}$$
$$- \underbrace{E\left\{\ln\left(1+\lambda N\mu_{i1}\frac{\gamma_{gi}}{\gamma_{21}\gamma_{1e}}\right)\right\}}_{I_{4(2)}} \quad (33)$$

Additionally, $I_{4(1)}$, and $I_{4(2)}$ are calculated in Appendix D which are equivalent (34) and (35) respectively, as follows:

$$I_{4(1)} = -\frac{\frac{\bar{\gamma}_{gi}}{\bar{\gamma}_{21}}\left(\ln\left(\frac{\bar{\gamma}_{gi}}{\bar{\gamma}_{21}}\right)-\ln\left(\frac{1}{\lambda N\mu_{i1}}\right)\right)}{-\frac{\bar{\gamma}_{gi}}{\bar{\gamma}_{21}}+\frac{1}{\lambda N\mu_{i1}}};$$
$$\frac{\bar{\gamma}_{gi}}{\bar{\gamma}_{21}} > 0, \quad \frac{1}{\lambda N\mu_{i1}} > 0 \quad (34)$$

$$I_{4(2)} = -\int_0^\infty \frac{\left(\frac{\bar{\gamma}_{gi}}{z\bar{\gamma}_{1e}\bar{\gamma}_{21}}e^{\frac{\bar{\gamma}_{gi}}{z\bar{\gamma}_{1e}\bar{\gamma}_{21}}}Ei\left(-\frac{\bar{\gamma}_{gi}}{z\bar{\gamma}_{1e}\bar{\gamma}_{21}}\right)\right)}{\left(z+\frac{1}{N\mu_{i1}}\right)}dz;$$
$$\frac{1}{z\bar{\gamma}_{1e}} > 0, \frac{\bar{\gamma}_{gi}}{\bar{\gamma}_{21}} > 0 \quad (35)$$

Hence, we rewrite (33) based on (34), and (35) as:

$$I_4 = I_{4(1)} - I_{4(2)}$$
$$= -\frac{\frac{\bar{\gamma}_{gi}}{\bar{\gamma}_{21}}\left(\ln\left(\frac{\bar{\gamma}_{gi}}{\bar{\gamma}_{21}}\right)-\ln\left(\frac{1}{\lambda N\mu_{i1}}\right)\right)}{-\frac{\bar{\gamma}_{gi}}{\bar{\gamma}_{21}}+\frac{1}{\lambda N\mu_{i1}}}$$
$$+ \int_0^\infty \frac{\left(\frac{\bar{\gamma}_{gi}}{z\bar{\gamma}_{1e}\bar{\gamma}_{21}}e^{\frac{\bar{\gamma}_{gi}}{z\bar{\gamma}_{1e}\bar{\gamma}_{21}}}Ei\left(-\frac{\bar{\gamma}_{gi}}{z\bar{\gamma}_{1e}\bar{\gamma}_{21}}\right)\right)}{\left(z+\frac{1}{N\mu_{i1}}\right)}dz;$$
$$\left\{\frac{\bar{\gamma}_{gi}}{\bar{\gamma}_{21}} > 0, \frac{1}{\lambda N\mu_{i1}} > 0; \frac{1}{z\bar{\gamma}_{1e}} > 0, \frac{\bar{\gamma}_{gi}}{\bar{\gamma}_{21}} > 0\right\}$$
$$(36)$$

IV. RESULT OF SIMULATION

In this section, the parameters of the simulation are illustrated in Table 1. Also, we assume that altitude of each communication link has Rayleigh fading distribution.

TABLE 1. Simulation parameters.

Parameter	description	value
N		8,16,64,128
λ		λ=1,10,15,20
P	Power transmission budget	1 W
κ		3

As shown in Fig. 2, IRS plates and BS because of problem assumptions and location of users (U_1, U_2, U_{Eve}), the value $\alpha = 0.7$ calculate to simulate results for the safe ratio at 23 Ghz central frequency and two legal users' channel conditions.

Fig 3, shows ESR versus ρ for three different locations of the U_{Eve}, case 1) near to IRS (ie) location $(-2, 2, 1.5)$, case 2) close to the first user (1e) location $(0, 0.6, 1.5)$, case 3) second U_{Eve} (2e) location $(1.5, 0.6, 1.5)$ for three different states Exa, Hig, and Asy which are defined respectively, as follows: case 1) Exa: refers to the exact results obtained from inserting relations (7) to (10) in relation (15). case 2) Hig: presents the simulation results at high SNR, which is obtained by inserting relations (16) to (19) in relation (15). case 3) Asy: is the simulation results in the asymptotic state, that is, when $\rho \to \infty$, and it is obtained by inserting the relations (16) to (19) in the relation (15), in the asymptotic state. In this figure, the number of BS antennas is 20, the number of IRS arrays is 64, and the BS power is 10 Watts. The U_{Eve} close to the IRS has the lowest secrecy rate compared to the other two cases, because the U_{Eve} receives the message with high power leading to a decrease in the ESR. Note that when the first user sends a data to the second user, if the U_{Eve} is closer to the first user, he receives U_2's information with more SNR
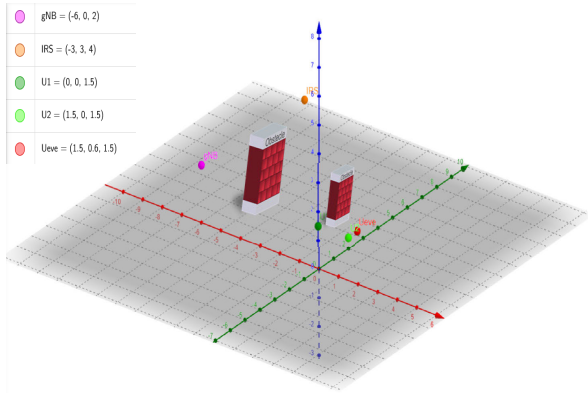
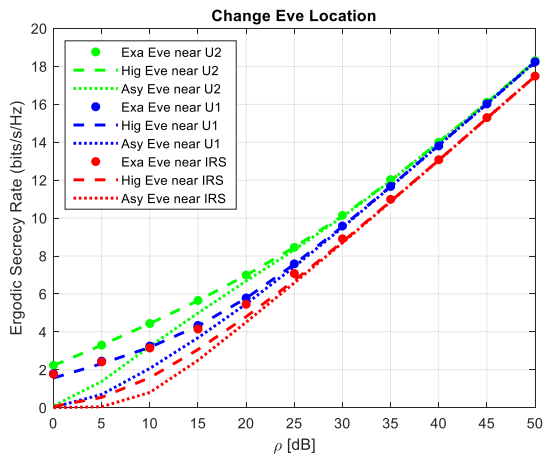**FIGURE 2.** Location of users (U_1, U_2, U_{Eve}), BS and IRS.

FIGURE 3. ESR versus transmit SNR (ρ), U_{Eve} is near to IRS, U_1 or U_2.

FIGURE 4. ESR versus ρ for different numbers of IRS elements when the U_{Eve} is near to U_2.

FIGURE 5. ESR versus number of BS antennas and analysis of BS transmit power.

FIGURE 6. Comparison performance between two orthogonal multiple access techniques, OMA and NOMA.

i.e, it decreases secrecy rate. When U_{Eve}'s position is close to the second user, the ESR is more than other situation. The reason is that, in this situation the U_{Eve} is farthest from the data transmitter and near to jamming transmitter which leads to increase ESR.

Fig. 4 illustrates the ESR versus ρ and analyze different values of elements of IRS when the U_{Eve} is close to the second user, in the cases of exact (Exa) and high SNR (Hig). By increasing IRS elements, the main beam of data signal can be focused on the U_1 which increase secrecy rate. As seen, the optimal and exact curves are perfectly matched which highlines our calculated equations are correct.

Fig. 5 shows ESR increases by increasing the number of BS antennas. The reason is that by increasing of number of antennas at BS, the main beam of data signal can be focused on IRS which increase secrecy rate. As seen in this figure, in high number of BS antennas the curves are saturated, because in this case increases of antennas it does not lead to a further increase in the main beam of data signal. Moreover, in high BS transmit power, the ESR changes very negligible. Hence, employing of very high antenna and transmit power at BS are not necessary in the proposed network.
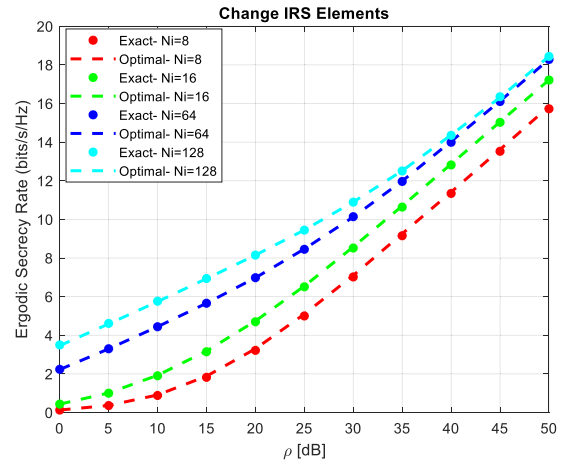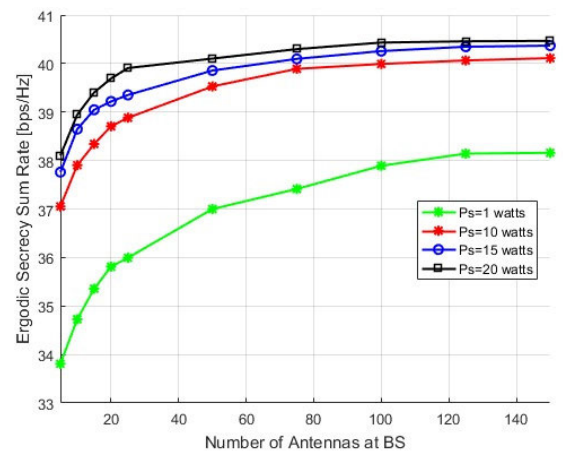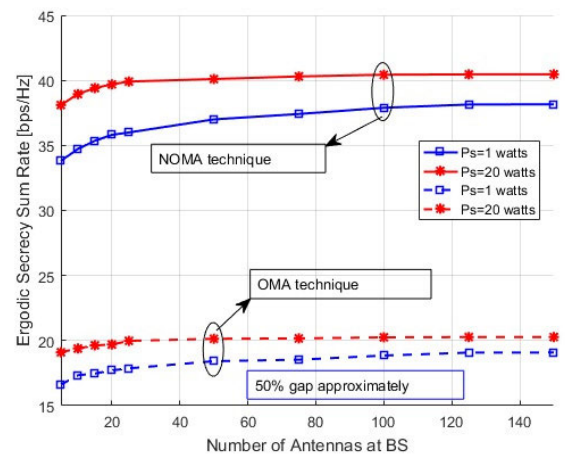
Fig 6 compared the performance of the OMA and NOMA techniques in the proposed system model. As shown in this figure, the NOMA technique provides 50% more ESR

compared to the OMA technique. As seen, high number of antennas at BS saturates the ESR, because in this case the U_{Eve} can benefits from high number of antennas. Consequently, in the proposed system model, 100 antenna is economical, because more than its ESR does not change.

V. CONCLUSION

In this paper, we analyzed a network consists a BS, two users, an IRS and an eavesdropper in an environment full of obstacles. In this network, due to the obstacles between users and BS there is not direct link between them. Hence, the communication is possible by employing the IRS. In addition, second user cannot communicate with an IRS due to an obstacle. To tackle this issue, we employed a new auxiliary path to keep the communication. In other words, first user is used as an amplify and forward relay to transmit second user's data. Moreover, to deceive eavesdropper, the second user which is idle in the second phase transmits jamming signal. To analyze the proposed system model, we obtained a closed-form for ESR. The numerical results reveals that increasing IRS elements can enhance the ESR, the reason is that increasing of IRS elements can focus the main beam of data signal on the first user which increase secrecy rate. Finally, we compared the performance of the OMA and NOMA techniques in the proposed system model. We showed that the NOMA technique provides 50% more ESR compared to the OMA technique.

APPENDIX A
CALCULATION OF I_2

$$I_{2(1)} = E\left\{\ln\left(1 + \lambda N\mu_{i1}\frac{\gamma_{gi}\gamma_{12}}{\gamma_{21}}\right)\right\}$$

$$= = E\left\{\ln\left(1 + \underbrace{\lambda N\mu_{i1}}_{\beta}\underbrace{\frac{\gamma_{gi}\gamma_{12}}{\gamma_{21}}}_{Z}\right)\right\}$$

$$F_Z(z) = Pr\{Z \le z\} = Pr\left\{\frac{\gamma_{gi}\gamma_{12}}{\gamma_{21}} \le z\right\}$$

$$= Pr\left\{\frac{\gamma_{gi}}{\gamma_{21}} \le \frac{z}{\gamma_{12}}\right\}$$

$$= E_\vartheta\left\{Pr\left\{\vartheta \le \frac{z}{\gamma_{12}} \mid \vartheta = \frac{\gamma_{gi}}{\gamma_{21}}\right\}\right\}$$

$$= = E_\vartheta\left\{\underbrace{pr\left\{\gamma_{12} \le \frac{z}{\vartheta} \mid \vartheta = \frac{\gamma_{gi}}{\gamma_{21}}\right\}}_{F_{\gamma_{12}}\left(\frac{z}{\vartheta}\right)}\right\}$$

$$= E_\vartheta\left\{F_{\gamma_{12}}\left(\frac{z}{\vartheta}\right)\right\}$$

$$F_{\gamma_{12}}\left(\frac{z}{\vartheta}\right) = \int_0^{\frac{z}{\vartheta}} f_{\gamma_{12}}(x)\,dx = \int_0^{\frac{z}{\vartheta}} \frac{1}{\bar{\gamma}_{12}}e^{-\frac{x}{\bar{\gamma}_{12}}}\,dx$$

$$= 1 - e^{-\frac{Z}{\vartheta\bar{\gamma}_{12}}}$$

$$F_Z(z) = E_\vartheta\left\{1 - e^{-\frac{Z}{\vartheta\bar{\gamma}_{12}}}\right\} = 1 - E_\vartheta\left\{e^{-\frac{Z}{\vartheta\bar{\gamma}_{12}}}\right\} \quad \text{(A.1)}$$

Assuming $\vartheta = \frac{\gamma_{gi}}{\gamma_{21}}$, γ_{gi} and γ_{21} have exponential distributions. The probability density function ϑ is calculated as:

$$f_\vartheta(x) = \frac{\partial}{\partial x}F_\vartheta(x) = \frac{\partial}{\partial x}(Pr\{\vartheta < x\})$$

$$= \underbrace{\frac{\partial}{\partial x}\int_0^\infty \int_0^{\beta x} f_{\gamma_{gi}}(\alpha)f_{\gamma_{21}}(\beta)\,d\alpha d\beta}_{c_1}$$

$$= \int_0^\infty \left(\frac{\partial}{\partial x}\int_0^{\beta x} f_{\gamma_{gi}}(\alpha)\,d\alpha\right)f_{\gamma_{21}}(\beta)\,d\beta$$

$$= \underbrace{\int_0^\infty \left(\beta f_{\gamma_{gi}}(\beta x)\right)f_{\gamma_{21}}(\beta)\,d\beta}_{c_2}$$

$$= \int_0^\infty \beta\left(\frac{1}{\bar{\gamma}_{gi}}e^{-\frac{\beta x}{\bar{\gamma}_{gi}}}\right)\left(\frac{1}{\bar{\gamma}_{21}}e^{-\frac{\beta}{\bar{\gamma}_{21}}}\right)\,d\beta$$

$$= \frac{1}{\bar{\gamma}_{gi}\bar{\gamma}_{21}}\int_0^\infty \beta e^{-\left(\frac{x\bar{\gamma}_{21}+\bar{\gamma}_{gi}}{\bar{\gamma}_{gi}\bar{\gamma}_{21}}\right)\beta}\,d\beta$$

$$= \underbrace{\frac{1}{\bar{\gamma}_{gi}\bar{\gamma}_{21}}\left(\frac{\bar{\gamma}_{gi}\bar{\gamma}_{21}}{x\bar{\gamma}_{21}+\bar{\gamma}_{gi}}\right)^2\Gamma(2)}_{c_3}$$

$$= \frac{\frac{\bar{\gamma}_{gi}}{\bar{\gamma}_{21}}}{\left(x+\frac{\bar{\gamma}_{gi}}{\bar{\gamma}_{21}}\right)^2};$$

$$Re\left(\frac{x\bar{\gamma}_{21}+\bar{\gamma}_{gi}}{\bar{\gamma}_{gi}\bar{\gamma}_{21}}\right) > 0, \quad Re(2) > 0$$

c_1 is derived based on independency of γ_{gi} and γ_{21}. c_2 follows the Leibniz integral rule [22, Eq. (0,410)]:

$$\frac{d}{dx}\int_{\psi(a)}^{\varphi(a)} f(x,a)\,dx = f(\varphi(a),a)\frac{d\varphi(a)}{da}$$

$$- f(\psi(a),a)\frac{d\psi(a)}{da}$$

$$+ \int_{\psi(a)}^{\varphi(a)} \frac{d}{da}f(x,a)\,dx$$

c_3 is derived by substituting PDFs γ_{gi} and γ_{21} into [Eq. (381, 4)] from the integrals book [25].

$$\int_0^\infty x^{\vartheta-1}e^{-\mu x}\,dx = \frac{1}{\mu^\vartheta}\Gamma(\vartheta); \{Re(\mu) > 0, Re(\vartheta) > 0\}$$

Therefore:

$$F_Z(z) \underbrace{=}_{c_4} 1 - \int_0^\infty e^{-\frac{z}{x\bar{\gamma}_{12}}}f_\vartheta(x)\,dx$$

$$\underbrace{=}_{c_5} 1 - \int_0^\infty e^{-\frac{z}{x\bar{\gamma}_{12}}}\frac{\frac{\bar{\gamma}_{gi}}{\bar{\gamma}_{21}}}{\left(x+\frac{\bar{\gamma}_{gi}}{\bar{\gamma}_{21}}\right)^2}\,dx$$

$$\underbrace{=}_{c_6} 1 - \left(\Gamma(1)e^{\frac{\bar{\gamma}_{21}z}{2\bar{\gamma}_{gi}\bar{\gamma}_{12}}}W_{-1,-\frac{1}{2}}(\frac{\bar{\gamma}_{21}z}{\bar{\gamma}_{gi}\bar{\gamma}_{12}})\right)$$

$$= 1 - \left(e^{\frac{\bar{\gamma}_{21}z}{2\bar{\gamma}_{gi}\bar{\gamma}_{12}}} W_{-1,-\frac{1}{2}} \left(\frac{\bar{\gamma}_{21}z}{\bar{\gamma}_{gi}\bar{\gamma}_{12}} \right) \right);$$
$$\left\{ \left| arg \left(\frac{\bar{\gamma}_{gi}}{\bar{\gamma}_{21}} \right) \right| < \pi, Re(2) > Re(1) > 0 \right\}$$

c_4 is derived from the expectation definition, c_5 is derived by substituting in the PDF $f_\vartheta(x)$, c_6 is derived using the equation. [22, Eq. (3.471.7)] of the integrals book where $W_{\lambda,\mu}(z)$ is Whittaker functions.

$$I_{2(1)} = E \left\{ ln \left(1 + \underbrace{\lambda N \mu_{i1}}_{\beta} \underbrace{\frac{\gamma_{gi}\gamma_{12}}{\gamma_{21}}}_{Z} \right) \right\}$$

$$= \int_0^\infty \frac{\beta(1 - F_Z(z))}{1 + \beta z} dz$$

$$= \int_0^\infty \frac{\lambda N \mu_{i1} \left(\left(e^{\frac{\bar{\gamma}_{21}z}{2\bar{\gamma}_{gi}\bar{\gamma}_{12}}} W_{-1,-\frac{1}{2}} \left(\frac{\bar{\gamma}_{21}z}{\bar{\gamma}_{gi}\bar{\gamma}_{12}} \right) \right) \right)}{1 + \lambda N \mu_{i1} z} dz;$$
$$\left\{ \left| arg \left(\frac{\bar{\gamma}_{gi}}{\bar{\gamma}_{21}} \right) \right| < \pi, Re(2) > Re(1) > 0 \right\}$$

Similar to $I_{2(1)}$ we can obtain $I_{2(2)}$ which are only different with the existence of α.

$$I_{2(2)} = E \left\{ ln \left(1 + \alpha \lambda N \mu_{i1} \frac{\gamma_{gi}\gamma_{12}}{\gamma_{21}} \right) \right\}$$

$$= \int_0^\infty \frac{\alpha \lambda N \mu_{i1} \left(\left(e^{\frac{\bar{\gamma}_{21}z}{2\bar{\gamma}_{gi}\bar{\gamma}_{12}}} W_{-1,-\frac{1}{2}} \left(\frac{\bar{\gamma}_{21}z}{\bar{\gamma}_{gi}\bar{\gamma}_{12}} \right) \right) \right)}{1 + \alpha \lambda N \mu_{i1} z} dz;$$
$$\left\{ \left| arg \left(\frac{\bar{\gamma}_{gi}}{\bar{\gamma}_{21}} \right) \right| < \pi, Re(2) > Re(1) > 0 \right\} \quad (A.2)$$

APPENDIX B
CALCULATION OF I_3

$$I_3 = E \left\{ ln \left(1 + \frac{\lambda \gamma_{e1g}}{N \mu_{i1} \gamma_{2e}} \right) \right\}$$

$$= E \left\{ ln \left(1 + \underbrace{\frac{\lambda}{N \mu_{i1}}}_{\alpha} \underbrace{\frac{\gamma_{e1g}}{\gamma_{2e}}}_{Z} \right) \right\}$$

$$F_Z(z) = Pr\{Z \le z\} = Pr \left\{ \frac{\gamma_{e1g}}{\gamma_{2e}} \le z \right\}$$

$$= Pr\{\gamma_{e1g} \le z \gamma_{2e}\}$$

$$= E_y \left\{ \underbrace{Pr\{\gamma_{e1g} \le zy \mid y = \gamma_{2e}\}}_{F_{\gamma_{e1g}}(zy)} \right\}$$

$$= E_y \{F_{\gamma_{e1g}}(zy)\}$$

$$F_{\gamma_{e1g}}(zy) = \int_0^{zy} f_{\gamma_{e1g}}(x) dx = \int_0^{zy} \frac{1}{\bar{\gamma}_{e1g}} e^{-\frac{x}{\bar{\gamma}_{e1g}}} dx$$

$$= \frac{1}{\bar{\gamma}_{e1g}} (-\bar{\gamma}_{e1g}) e^{-\frac{x}{\bar{\gamma}_{e1g}}} \Big|_0^{zy}$$

$$= - \left(e^{-\frac{zy}{\bar{\gamma}_{e1g}}} - e^0 \right)$$

$$= 1 - e^{-\frac{zy}{\bar{\gamma}_{e1g}}}$$

$$F_Z(z) = E_y \left\{ 1 - e^{-\frac{zy}{\bar{\gamma}_{e1g}}} \right\} 1 - \int_0^\infty e^{-\frac{zy}{\bar{\gamma}_{e1g}}} f_Y(y) dy$$

$$\underset{c_2}{=} 1 - \int_0^\infty e^{-\frac{zy}{\bar{\gamma}_{e1g}}} \frac{1}{\bar{\gamma}_{2e}} e^{-\frac{y}{\bar{\gamma}_{2e}}} dy$$

$$= 1 - \int_0^\infty e^{\left(-\frac{z}{\bar{\gamma}_{e1g}} - \frac{1}{\bar{\gamma}_{2e}} \right) y} \frac{1}{\bar{\gamma}_{2e}} dy$$

$$= 1 - \frac{\bar{\gamma}_{e1g}}{z\bar{\gamma}_{2e} + \bar{\gamma}_{e1g}}$$

c_1 is derived using the mathematical expectation definition and c_2 is derived by employing the probability density function γ_{2e}.

$$I_3 = E \left\{ ln \left(1 + \underbrace{\frac{\lambda}{N \mu_{i1}}}_{\alpha} \underbrace{\frac{\bar{\gamma}_{e1g}}{\gamma_{2e}}}_{Z} \right) \right\}$$

$$= \int_0^\infty \frac{\alpha(1 - F_Z(z))}{1 + \alpha z} dz$$

$$= \int_0^\infty \frac{\frac{\lambda}{N \mu_{i1}} \left(1 - 1 + \frac{\bar{\gamma}_{e1g}}{z\bar{\gamma}_{2e} + \bar{\gamma}_{e1g}} \right)}{1 + \frac{\lambda}{N \mu_{i1}} z} dz$$

$$= \int_0^\infty \frac{\frac{\lambda}{N \mu_{i1}} \bar{\gamma}_{e1g}}{(z\bar{\gamma}_{2e} + \bar{\gamma}_{e1g}) \left(1 + \frac{\lambda}{N \mu_{i1}} z \right)} dz$$

$$= \int_0^\infty \frac{\frac{\lambda}{N \mu_{i1}} \frac{\bar{\gamma}_{e1g}}{\bar{\gamma}_{2e}}}{\left(z + \frac{\bar{\gamma}_{e1g}}{\bar{\gamma}_{2e}} \right) \left(1 + \frac{\lambda}{N \mu_{i1}} z \right)} dz$$

$$= \int_0^\infty \frac{\frac{\bar{\gamma}_{e1g}}{\bar{\gamma}_{2e}}}{\left(z + \frac{\bar{\gamma}_{e1g}}{\bar{\gamma}_{2e}} \right) \left(\frac{N \mu_{i1}}{\lambda} + z \right)} dz$$

$$= -\frac{\frac{\bar{\gamma}_{e1g}}{\bar{\gamma}_{2e}} \left(ln \left(\frac{\bar{\gamma}_{e1g}}{\bar{\gamma}_{2e}} \right) - ln \left(\frac{N \mu_{i1}}{\lambda} \right) \right)}{-\frac{\bar{\gamma}_{e1g}}{\bar{\gamma}_{2e}} + \frac{N \mu_{i1}}{\lambda}};$$

$$\frac{\bar{\gamma}_{e1g}}{\bar{\gamma}_{2e}} > 0, \frac{N \mu_{i1}}{\lambda} > 0 \quad (B.1)$$

$$I_3 = -\frac{\frac{\bar{\gamma}_{e1g}}{\bar{\gamma}_{2e}} \left(ln \left(\frac{\bar{\gamma}_{e1g}}{\bar{\gamma}_{2e}} \right) - ln \left(\frac{N \mu_{i1}}{\lambda} \right) \right)}{-\frac{\bar{\gamma}_{e1g}}{\bar{\gamma}_{2e}} + \frac{N \mu_{i1}}{\lambda}};$$

$$\frac{\bar{\gamma}_{e1g}}{\bar{\gamma}_{2e}} > 0, \frac{N \mu_{i1}}{\lambda} > 0 \quad (B.2)$$

APPENDIX C
CALCULATION OF I_4

$$I_4 = \mathrm{E}\left\{\ln\left(1 + \frac{\lambda N \mu_{i1}\gamma_{gi}\gamma_{1e}}{\gamma_{21}\gamma_{1e} + \gamma_{1e} + \lambda N \mu_{i1}\gamma_{gi} + \gamma_{21}}\right)\right\} \quad (C.1)$$

$$= \mathrm{E}\left\{\ln\left(\frac{\gamma_{21}\gamma_{1e} + \gamma_{1e} + \lambda N \mu_{i1}\gamma_{gi} + \gamma_{21} + \lambda N \mu_{i1}\gamma_{gi}\gamma_{1e}}{\gamma_{21}\gamma_{1e} + \gamma_{1e} + \lambda N \mu_{i1}\gamma_{gi} + \gamma_{21}}\right)\right\}$$

$$\cong E\left\{\ln\left(\frac{\gamma_{21}\gamma_{1e} + \lambda N \mu_{i1}\gamma_{gi}\gamma_{1e}}{\gamma_{21}\gamma_{1e} + \lambda N \mu_{i1}\gamma_{gi}}\right)\right\}$$

$$= \mathrm{E}\left\{\ln\left(\gamma_{21}\gamma_{1e} + \lambda N \mu_{i1}\gamma_{gi}\gamma_{1e}\right)\right\}$$
$$\quad - \mathrm{E}\left\{\ln\left(\gamma_{21}\gamma_{1e} + \lambda N \mu_{i1}\gamma_{gi}\right)\right\}$$

$$= \mathrm{E}\left\{\ln\left(\gamma_{21}\gamma_{1e}\left(1 + \lambda N \mu_{i1}\frac{\gamma_{gi}}{\gamma_{21}}\right)\right)\right\}$$
$$\quad - \mathrm{E}\left\{\ln\left(\gamma_{21}\gamma_{1e}\left(1 + \lambda N \mu_{i1}\frac{\gamma_{gi}}{\gamma_{21}\gamma_{1e}}\right)\right)\right\} \quad (C.2)$$

APPENDIX D
CALCULATION OF I_4

Similar to calculation of I_3 in Appendix C, we derive the $I_{4(1)}$ as follow as:

$$I_{4(1)} = E\left\{\ln\left(1 + \lambda N \mu_{i1}\frac{\gamma_{gi}}{\gamma_{21}}\right)\right\}$$

$$= -\frac{\frac{\bar{\gamma}_{gi}}{\bar{\gamma}_{21}}\left(\ln\left(\frac{\bar{\gamma}_{gi}}{\bar{\gamma}_{21}}\right) - \ln\left(\frac{1}{\lambda N \mu_{i1}}\right)\right)}{-\frac{\bar{\gamma}_{gi}}{\bar{\gamma}_{21}} + \frac{1}{\lambda N \mu_{i1}}};$$
$$\frac{\bar{\gamma}_{gi}}{\bar{\gamma}_{21}} > 0, \frac{1}{\lambda N \mu_{i1}} > 0 \quad (D.1)$$

Also, $I_{4(2)}$ obtained as expressed

$$I_{4(2)} = E\left\{\ln\left(1 + \lambda N \mu_{i1}\frac{\gamma_{gi}}{\gamma_{21}\gamma_{1e}}\right)\right\}$$

$$= E\left\{\ln\left(1 + \underbrace{\lambda N \mu_{i1}}_{\beta}\underbrace{\frac{\gamma_{gi}}{\gamma_{21}\gamma_{1e}}}_{Z}\right)\right\}$$

$$F_Z(z) = pr\{Z \le z\} = pr\left\{\frac{\gamma_{gi}}{\gamma_{21}\gamma_{1e}} \le z\right\}$$

$$= pr\left\{\frac{\gamma_{gi}}{\gamma_{21}} \le z\gamma_{1e}\right\}$$

$$= E_\vartheta\left\{pr\left\{\vartheta \le z\gamma_{1e} \mid \vartheta = \frac{\gamma_{gi}}{\gamma_{21}}\right\}\right\}$$

$$= E_\vartheta\left\{pr\left\{\gamma_{1e} \ge \frac{\vartheta}{z} \mid \vartheta = \frac{\gamma_{gi}}{\gamma_{21}}\right\}\right\}$$

$$= E_\vartheta\left\{1 - pr\left\{\gamma_{1e} \le \frac{\vartheta}{z} \mid \vartheta = \frac{\gamma_{gi}}{\gamma_{21}}\right\}\right\}$$

$$= 1 - E_\vartheta\left\{\underbrace{pr\left\{\gamma_{1e} \le \frac{\vartheta}{z} \;\middle|\; \vartheta = \frac{\gamma_{gi}}{\gamma_{21}}\right\}}_{F_{\gamma_{1e}}\left(\frac{\vartheta}{z}\right)}\right\}$$

$$= 1 - E_\vartheta\left\{F_{\gamma_{1e}}\left(\frac{\vartheta}{z}\right)\right\}$$

$$F_{\gamma_{1e}}\left(\frac{\vartheta}{z}\right) = \int_0^{\frac{\vartheta}{z}} f_{\gamma_{1e}}(x)\, dx = \int_0^{\frac{\vartheta}{z}} \frac{1}{\bar{\gamma}_{1e}} e^{-\frac{x}{\bar{\gamma}_{1e}}}\, dx$$

$$= 1 - e^{-\frac{\vartheta}{z\bar{\gamma}_{1e}}}$$

$$F_Z(z) = E_\vartheta\left\{e^{-\frac{\vartheta}{z\bar{\gamma}_{1e}}}\right\} \quad (D.2)$$

Assuming $\vartheta = \frac{\gamma_{gi}}{\gamma_{21}}$, γ_{gi} and γ_{21} have exponential distributions. The probability density function ϑ is calculated as:

$$f_\vartheta(x) = \frac{\partial}{\partial x}F_\vartheta(x) = \frac{\partial}{\partial x}(\mathrm{Pr}\{\vartheta < x\})$$

$$\underbrace{=}_{c_1} \frac{\partial}{\partial x}\int_0^\infty \int_0^{\beta x} f_{\gamma_{gi}}(\alpha) f_{\gamma_{21}}(\beta)\, d\alpha\, d\beta$$

$$= \int_0^\infty \left(\frac{\partial}{\partial x}\int_0^{\beta x} f_{\gamma_{gi}}(\alpha)\, d\alpha\right) f_{\gamma_{21}}(\beta)\, d\beta$$

$$\underbrace{=}_{c_2} \int_0^\infty \left(\beta f_{\gamma_{gi}}(\beta x)\right) f_{\gamma_{21}}(\beta)\, d\beta$$

$$= \int_0^\infty \beta\left(\frac{1}{\bar{\gamma}_{gi}}e^{-\frac{\beta x}{\bar{\gamma}_{gi}}}\right)\left(\frac{1}{\bar{\gamma}_{21}}e^{-\frac{\beta}{\bar{\gamma}_{21}}}\right)\, d\beta$$

$$= \frac{1}{\bar{\gamma}_{gi}\bar{\gamma}_{21}}\int_0^\infty \beta e^{-\left(\frac{x\bar{\gamma}_{21} + \bar{\gamma}_{gi}}{\bar{\gamma}_{gi}\bar{\gamma}_{21}}\right)\beta}\, d\beta$$

$$\underbrace{=}_{c_3} \frac{1}{\bar{\gamma}_{gi}\bar{\gamma}_{21}}\left(\frac{\bar{\gamma}_{gi}\bar{\gamma}_{21}}{x\bar{\gamma}_{21} + \bar{\gamma}_{gi}}\right)^2 \Gamma(2)$$

$$= \frac{\frac{\bar{\gamma}_{gi}}{\bar{\gamma}_{21}}}{\left(x + \frac{\bar{\gamma}_{gi}}{\bar{\gamma}_{21}}\right)^2};$$
$$Re\left(\frac{x\bar{\gamma}_{21} + \bar{\gamma}_{gi}}{\bar{\gamma}_{gi}\bar{\gamma}_{21}}\right) > 0, \quad Re(2) > 0$$

c_1 is derived based on independency of γ_{gi} and γ_{21}. c_2 follows the Leibniz integral rule [22, Eq. (0.410)]:

$$\frac{d}{dx}\int_{\psi(a)}^{\varphi(a)} f(x, a)\, dx = f(\varphi(a), a)\frac{d\varphi(a)}{da}$$
$$- f(\psi(a), a)\frac{d\psi(a)}{da}$$
$$+ \int_{\psi(a)}^{\varphi(a)} \frac{d}{da}f(x, a)\, dx$$

c_3 is derived by substituting PDFs γ_{gi} and γ_{21} into [Eq. (3.381.4)] from the integrals book [25].

$$\int_0^\infty x^{\vartheta - 1}e^{-\mu x}\, dx = \frac{1}{\mu^\vartheta}\Gamma(\vartheta); \{Re(\mu) > 0, Re(\vartheta) > 0\}$$

Therefore:

$$F_Z(z) \underbrace{=}_{c_4} \int_0^\infty e^{-\frac{\vartheta}{z\bar{\gamma}_{1e}}} f_\vartheta(x)\, dx$$

$$\underset{c_5}{=} \int_0^\infty e^{-\frac{x}{z\bar{\gamma}_{1e}}} \frac{\frac{\bar{\gamma}_{gi}}{\bar{\gamma}_{21}}}{\left(x + \frac{\bar{\gamma}_{gi}}{\bar{\gamma}_{21}}\right)^2} dx$$

$$\underset{c_6}{=} \frac{\bar{\gamma}_{gi}}{\bar{\gamma}_{21}}\left(\frac{1}{z\bar{\gamma}_{1e}} e^{\frac{\bar{\gamma}_{gi}}{z\bar{\gamma}_{1e}\bar{\gamma}_{21}}} Ei\left(-\frac{\bar{\gamma}_{gi}}{z\bar{\gamma}_{1e}\bar{\gamma}_{21}}\right) + \frac{\bar{\gamma}_{21}}{\bar{\gamma}_{gi}}\right)$$

$$= \frac{\bar{\gamma}_{gi}}{z\bar{\gamma}_{1e}\bar{\gamma}_{21}} e^{\frac{\bar{\gamma}_{gi}}{z\bar{\gamma}_{1e}\bar{\gamma}_{21}}} Ei\left(-\frac{\bar{\gamma}_{gi}}{z\bar{\gamma}_{1e}\bar{\gamma}_{21}}\right) + 1;$$

$$\left\{\frac{1}{z\bar{\gamma}_{1e}} > 0, \frac{\bar{\gamma}_{gi}}{\bar{\gamma}_{21}} > 0\right\}$$

c_4 is derived from the expectation definition, c_5 is derived by substituting in the PDF $f_\vartheta(x)$, c_6 is derived using the equation. [22, Eq. (3.353.3)] of the integrals book.

$$I_{4(2)}$$

$$= E\left\{ln\left(1 + \underbrace{\lambda N\mu_{i1}}_{\beta} \underbrace{\frac{\gamma_{gi}}{\gamma_{21}\gamma_{1e}}}_{z}\right)\right\}$$

$$= \int_0^\infty \frac{\beta(1 - F_Z(z))}{1 + \beta z} dz$$

$$= \int_0^\infty \frac{\lambda N\mu_{i1}\left(1 - \left(\frac{\bar{\gamma}_{gi}}{z\bar{\gamma}_{1e}\bar{\gamma}_{21}} e^{\frac{\bar{\gamma}_{gi}}{z\bar{\gamma}_{1e}\bar{\gamma}_{21}}} Ei\left(-\frac{\bar{\gamma}_{gi}}{z\bar{\gamma}_{1e}\bar{\gamma}_{21}}\right) + 1\right)\right)}{1 + \lambda N\mu_{i1}z} dz$$

$$= -\int_0^\infty \frac{\left(\frac{\bar{\gamma}_{gi}}{z\bar{\gamma}_{1e}\bar{\gamma}_{21}} e^{\frac{\bar{\gamma}_{gi}}{z\bar{\gamma}_{1e}\bar{\gamma}_{21}}} Ei\left(-\frac{\bar{\gamma}_{gi}}{z\bar{\gamma}_{1e}\bar{\gamma}_{21}}\right)\right)}{\left(z + \frac{1}{N\mu_{i1}}\right)} dz;$$

$$\frac{1}{z\bar{\gamma}_{1e}} > 0, \frac{\bar{\gamma}_{gi}}{\bar{\gamma}_{21}} > 0$$

REFERENCES

[1] L. Dai, B. Wang, Z. Ding, Z. Wang, S. Chen, and L. Hanzo, "A survey of non-orthogonal multiple access for 5G," *IEEE Commun. Surveys Tuts.*, vol. 20, no. 3, pp. 2294–2323, 3rd Quart., 2018.

[2] W. Shin, M. Vaezi, B. Lee, D. J. Love, J. Lee, and H. V. Poor, "Non-orthogonal multiple access in multi-cell networks: Theory, performance, and practical challenges," *IEEE Commun. Mag.*, vol. 55, no. 10, pp. 176–183, Oct. 2017, doi: 10.1109/MCOM.2017.1601065.

[3] Y. Qi and M. Vaezi, "Secure transmission in MIMO-NOMA networks," *IEEE Commun. Lett.*, vol. 24, no. 12, pp. 2696–2700, Dec. 2020.

[4] Z. Zhang, C. Zhang, C. Jiang, F. Jia, J. Ge, and F. Gong, "Improving physical layer security for reconfigurable intelligent surface aided NOMA 6G networks," *IEEE Trans. Veh. Technol.*, vol. 70, no. 5, pp. 4451–4463, May 2021, doi: 10.1109/TVT.2021.3068774.

[5] Q. Wu and R. Zhang, "Towards smart and reconfigurable environment: Intelligent reflecting surface aided wireless network," *IEEE Commun. Mag.*, vol. 58, no. 1, pp. 106–112, Jan. 2020.

[6] J. Chen, Y. Liang, Y. Pei, and H. Guo, "Intelligent reflecting surface: A programmable wireless environment for physical layer security," *IEEE Access*, vol. 7, pp. 82599–82612, 2019.

[7] J. Zhao, "A survey of intelligent reflecting surfaces (IRSs): Towards 6G wireless communication networks," 2019, *arXiv:1907.04789*.

[8] Z. Tang, T. Hou, Y. Liu, J. Zhang, and L. Hanzo, "Physical layer security of intelligent reflective surface aided NOMA networks," *IEEE Trans. Veh. Technol.*, vol. 71, no. 7, pp. 7821–7834, Jul. 2022, doi: 10.1109/TVT.2022.3168392.

[9] W. Wang, Y. Cao, M. Sheng, J. Tang, N. Zhao, D. Niyato, and K. Wong, "Secure beamforming for IRS-enhanced NOMA networks," *IEEE Wireless Commun.*, vol. 30, no. 1, pp. 134–140, Feb. 2023, doi: 10.1109/MWC.012.2100639.

[10] Y. Qi and M. Vaezi, "IRS-assisted physical layer security in MIMO-NOMA networks," *IEEE Commun. Lett.*, vol. 27, no. 3, pp. 792–796, Mar. 2023, doi: 10.1109/LCOMM.2023.3235722.

[11] C. Huang, G. Chen, and K. Wong, "Multi-agent reinforcement learning-based buffer-aided relay selection in IRS-assisted secure cooperative networks," *IEEE Trans. Inf. Forensics Security*, vol. 16, pp. 4101–4112, 2021, doi: 10.1109/TIFS.2021.3103062.

[12] A. Kuhestani, A. Mohammadi, and M. Mohammadi, "Joint relay selection and power allocation in large-scale MIMO systems with untrusted relays and passive eavesdroppers," *IEEE Trans. Inf. Forensics Security*, vol. 13, no. 2, pp. 341–355, Feb. 2018.

[13] J. Lim, T. Kim, and I. Bang, "Impact of outdated CSI on the secure communication in untrusted in-band full-duplex relay networks," *IEEE Access*, vol. 10, pp. 19825–19835, 2022, doi: 10.1109/ACCESS.2022.3151792.

[14] B. He, X. Zhou, and T. D. Abhayapala, "Achieving secrecy without knowing the number of eavesdropper antennas," *IEEE Trans. Wireless Commun.*, vol. 14, no. 12, pp. 7030–7043, Dec. 2015.

[15] S. Goel and R. Negi, "Guaranteeing secrecy using artificial noise," *IEEE Trans. Wireless Commun.*, vol. 7, no. 6, pp. 2180–2189, Jun. 2008.

[16] X. Zhou and M. R. McKay, "Secure transmission with artificial noise over fading channels: Achievable rate and optimal power allocation," *IEEE Trans. Veh. Technol.*, vol. 59, no. 8, pp. 3831–3842, Oct. 2010.

[17] L. Yang, J. Yang, W. Xie, M. O. Hasna, T. Tsiftsis, and M. D. Renzo, "Secrecy performance analysis of RIS-aided wireless communication systems," *IEEE Trans. Veh. Technol.*, vol. 69, no. 10, pp. 12296–12300, Oct. 2020.

[18] H. Shen, W. Xu, S. Gong, Z. He, and C. Zhao, "Secrecy rate maximization for intelligent reflecting surface assisted multi-antenna communications," *IEEE Commun. Lett.*, vol. 23, no. 9, pp. 1488–1492, Sep. 2019.

[19] L. Dong and H. Wang, "Secure MIMO transmission via intelligent reflecting surface," *IEEE Wireless Commun. Lett.*, vol. 9, no. 6, pp. 787–790, Jun. 2020.

[20] S. Hong, C. Pan, H. Ren, K. Wang, and A. Nallanathan, "Artificial-noise-aided secure MIMO wireless communications via intelligent reflecting surface," *IEEE Trans. Commun.*, vol. 68, no. 12, pp. 7851–7866, Dec. 2020.

[21] B. Feng, Y. Wu, and M. Zheng, "Secure transmission strategy for intelligent reflecting surface enhanced wireless system," in *Proc. 11th Int. Conf. Wireless Commun. Signal Process. (WCSP)*, Oct. 2019, pp. 1–6.

[22] C. Zhang, F. Jia, Z. Zhang, J. Ge, and F. Gong, "Physical layer security designs for 5G NOMA systems with a stronger near-end internal eavesdropper," *IEEE Trans. Veh. Technol.*, vol. 69, no. 11, pp. 13005–13017, Nov. 2020.

[23] M. Alageli, A. Ikhlef, F. Alsifiany, M. A. M. Abdullah, G. Chen, and J. Chambers, "Optimal downlink transmission for cell-free SWIPT massive MIMO systems with active eavesdropping," *IEEE Trans. Inf. Forensics Security*, vol. 15, pp. 1983–1998, 2020.

[24] J. Wang, J. Lee, F. Wang, and T. Q. S. Quek, "Jamming-aided secure communication in massive MIMO Rician channels," *IEEE Trans. Wireless Commun.*, vol. 14, no. 12, pp. 6854–6868, Dec. 2015.

[25] A. Jeffrey and D. Zwillinger, *Gradshteyn and Ryzhik's Table of Integrals, Series, and Products*, 7th ed. New York, NY, USA: Academic, 2007.

AFSHIN SOUZANI received the master's degree in electrical engineering (telecommunication) from the Science and Research Branch, Islamic Azad University, Tehran, Iran, in 2006, where he is currently pursuing the Ph.D. degree in electrical engineering (telecommunication). His current research interests include modulation and coding techniques, digital signal processing, wireless communications, resource allocation, estimation, and detection theories.

MOHAMMAD ALI POURMINA received the Ph.D. degree in electrical engineering (telecommunication) from the Science and Research Branch, Islamic Azad University, Tehran, Iran, in 1996. In 1996, he joined Islamic Azad University, where he was a Top Professor, in 2016. He is currently an Associate Professor of electrical engineering (telecommunication) with the Science and Research Branch, Islamic Azad University. Since 1991, he has been performing research in the areas of packet radio networks and digital signal processing systems. His current research interests include spread-spectrum systems, cellular mobile communications, indoor wireless communications, digital signal processing processors, and wireless multimedia networks. Since 1992, he has been a member of the Iran Telecommunication Research Center.
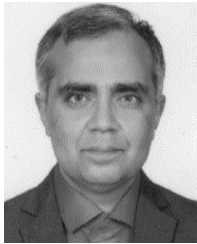
PAEIZ AZMI (Senior Member, IEEE) was born in Tehran, Iran, in 1974. He received the B.Sc., M.Sc., and Ph.D. degrees in electrical engineering from the Sharif University of Technology, Tehran, in 1996, 1998, and 2002, respectively. From 1999 to 2001, he was with the Advanced Communication Science Research Laboratory, Iran Telecommunication Research Center (ITRC), Tehran. From 2002 to 2005, he was with the Signal Processing Research Group, ITRC. Since September 2002, he has been with the Department of Electrical and Computer Engineering, Tarbiat Modares University, Tehran, where he became an Associate Professor, in January 2006, and currently a Full Professor. His current research interests include modulation and coding techniques, digital signal processing, wireless communications, resource allocation, molecular communications, and estimation and detection theories.

MOHAMMAD NASER-MOGHADASI was born in Saveh, Iran, in 1959. He received the B.Sc. degree in communication engineering from Leeds Metropolitan University (formerly Leeds Polytechnic), Leeds, U.K., in 1985, and the Ph.D. degree from the University of Bradford, Bradford, U.K., in 1993. From 1985 to 1987, he was an RF Design Engineer with Gigatech Company, Newcastle upon Tyne, U.K. He was offered two years postdoctoral position with the University of Nottingham, U.K., to pursue research on microwave cooking of materials. In 1995, he joined the Science and Research Branch, Islamic Azad University, Iran, where he is currently an Associate Professor and the Head of the Telecommunication Group. He has published more than 160 papers in different journals and conferences. His main research interests include microstrip antenna, microwave passive and active circuits, and RF MEMS. He is a member of the Institution of Engineering and Technology and the Institute of Electronics, Information and Communication Engineers. From 1987 to 1989, he was awarded a full scholarship by the Leeds Educational Authority to pursue the M.Phil. degree in CAD of microwave circuits.

● ● ●